Biochemical Pharmacology, Vol. 59, pp. 1187–1201, 2000.

ISSN 0006-2952/00/$–see front matter
PII S0006-2952(00)00245-8

Transport of Cyclic AMP and Synthetic Analogs in the Perfused Rat Liver

*Geraldo Emílio Vicentini, Jorgete Constantin, Carlos Henrique Lopez and Adelar Bracht**

LABORATORY OF LIVER METABOLISM, UNIVERSITY OF MARINGÁ, 87.020.900 MARINGÁ, BRAZIL

ABSTRACT. The purpose of the present work was to investigate the transport of cyclic AMP (cAMP) and analogs in the rat liver. The experimental system was the isolated once-through perfused liver. Transport was measured by employing the multiple-indicator dilution technique. The single-pass recovery of tracer [^{32}P]cAMP was equal to 94.4 ± 1.4%; no significant extracellular transformation of cAMP occurred during a single passage. The unidirectional influx rates of dibutyryl-cAMP were a saturable function of its concentration, with K_m = 72.75 ± 9.24 μM and V_{max} = 0.464 ± 0.026 μmol min^{-1} (mL cellular space)$^{-1}$. The unidirectional influx rates of cAMP were much lower than those of dibutyryl-cAMP and were a linear function of the concentration (up to 100 μM). The transfer coefficient for influx (k_{in}) was equal to 0.860 ± 0.058 mL min^{-1} (mL extracellular space)$^{-1}$. cAMP inhibited the influx of dibutyryl-cAMP; the IC_{50} was 0.83 mM. The following series of increasing unidirectional influx rates was found: cAMP < monobutyryl-cAMP ≈ 2-*aza*-ε-cAMP < *rp*-cAMPS ≈ *sp*-cAMPS < 8-Br-cAMP ≈ dibutyryl-cGMP ≈ 8-Cl-cAMP < *O*-dibutyryl-cAMP. There was no precise correlation between the rates of influx of the various cyclic nucleotides and their lipophilicity. It was concluded that the penetration of cAMP and its analogs into the liver cells was a facilitated process. Lipophilicity was not the only factor determining the rate of transport. The transformation of dibutyryl-cAMP was limited by both transport and activity of the intracellular enzymic systems. The intracellular transformation of exogenous cAMP, however, was limited by the transport process. BIOCHEM PHARMACOL **59**;10:1187–1201, 2000. © 2000 Elsevier Science Inc.

KEY WORDS. rat liver; multiple-indicator dilution; cAMP; transport; extracellular hydrolysis

Despite the wealth of information on cAMP† and its many roles in metabolism, its transport across membranes has been the subject of only a few studies. There are some intrinsic difficulties associated with the measurement of cAMP transport in isolated cell systems: (a) the compound can be hydrolyzed extra- and intracellularly to compounds that can undergo further transformations and translocations; and (b) the rate of permeation in most cells seems to be relatively low. The problem of cAMP metabolic transformation was overcome by Holman [1] by using human erythrocyte ghosts. In this system, cAMP permeates the cell membrane at appreciable rates with saturation of influx and efflux and inhibition by cytochalasin B. The system also showed counterflow, and Holman [1] proposed the existence of a transport system for cAMP.

In the liver, there are several indications that cAMP permeates the cell membrane. It has long been known that liver cells, as well as many other animal cells, are able to release cAMP when stimulated by glucagon and other hormones [2]. This means that liver cells are permeable to cAMP, at least in the efflux direction. Kagimoto and Uyeda [3] have reported that in the once-through perfused liver, 100 μM cAMP induces phosphofructokinase phosphorylation to an extent equal to that produced by saturating glucagon. The intracellular cAMP content under these conditions is equal to 2.5 nmol/g liver (~4.2 μM), which corresponds to a 3-fold increase relative to the basal levels. Levine *et al.* [4] have found labeled cAMP in bile after perfusing the liver with [8-^{14}C]cAMP. Those authors interpreted this finding as evidence that cAMP is able to traverse the hepatic cells. Furthermore, as reported by Constantin *et al.* [5], the metabolic actions of 50 μM cAMP, 100 μM N^6-monobutyryl-cAMP, and 100 μM N^6,2′-*O*-dibutyryl-cAMP on glycogenolysis, glycolysis, and oxygen uptake in the once-through perfused rat liver are practically the same and are comparable to those of glucagon.

In spite of all these findings, direct measurements of cAMP transport have not been done until now, so that the rate at which cAMP permeates the cell membrane is still unknown. Data are also lacking for the cAMP analogs,

* Corresponding author: Dr. Adelar Bracht, Laboratory of Liver Metabolism, Department of Biochemistry, University of Maringá, 87.020.900 Maringá, Brazil. FAX (44) 261-4396; E-mail: abracht@pbc.uem.br

† *Abbreviations*: cAMP, cyclic AMP; 2-*aza*-ε-cAMP, 2-*aza*-1,N^6-ethenoadenosine-3′,5′-cyclic monophosphate; 8-Br-cAMP, 8-bromoadenosine-3′,5′-cyclic monophosphate; 8-Cl-cAMP, 8-chloroadenosine-3′,5′-cyclic monophosphate; *rp*-cAMPS, *rp*-isomer of adenosine-3′,5′-cyclic monophosphorothioate; and *sp*-cAMPS, *sp*-isomer of adenosine-3′,5′-cyclic monophosphorothioate.

Received 27 July 1999; accepted 22 September 1999.

which have been used frequently in many kinds of experiments. For this reason, it seems worthwhile to develop a method for measuring cAMP transport in the liver. A suitable method for this purpose could be the multiple-indicator dilution technique using [^{32}P]cAMP [6, 7]. This technique has the advantage of allowing the measurement of transport in the intact organ, where only a limited portion of the cell surface is exposed, without the redistribution of enzyme and transport activities that normally occurs when hepatocytes are isolated. And, by using [^{32}P]cAMP, only two labeled products can be expected to be produced extracellularly: [^{32}P]AMP and [^{32}P]phosphate. Both can be eliminated easily and selectively from the samples by precipitation with nascently formed $Zn(OH)_2 \cdot BaSO_4$ [8]. [^{32}P]Phosphate should largely predominate in the perfusate, due to the rapid extracellular hydrolysis of AMP [9]. Inorganic phosphate permeates the liver cell membranes at very low rates. As shown elsewhere, the outflow profiles of labeled phosphate in hemoglobin- and substrate-free perfused livers cannot be distinguished from those of [^{14}C]sucrose, a marker for the extracellular space [10, 11]. Furthermore, most mammalian cells are practically impermeable to non-cyclic adenine nucleotides [12]. Only specialized structures, such as the synaptosomes, for example, possess transport systems for AMP [13]. For these reasons, if extracellular hydrolysis of [^{32}P]cAMP is significant during a single passage through the liver, this should be revealed by the presence of [^{32}P]phosphate and [^{32}P]AMP. Based on these principles, we have investigated the transport of [^{32}P]cAMP in the isolated perfused rat liver. The transport of several analogs, especially [^{3}H]dibutyryl-cAMP, was also investigated. The extension of the experiments to the analogs should be useful for comparative and mechanistic purposes.

MATERIALS AND METHODS

Materials

The liver perfusion apparatus and the rapid sampling apparatus for multiple-indicator dilution experiments were built in the workshops of the University of Maringá [7, 10]. [^{32}P]Adenosine 3′,5′-cyclic monophosphate ([^{32}P]cAMP; specific activity 25 Ci/mmol) was purchased from ICN Pharmaceutical, Inc. [2,8-^{3}H]N^6,2′-*O*-Dibutyryl-3′,5′-cAMP (8.9 Ci/mmol) was a custom preparation from Moravek Biochemicals. [U-^{14}C]Sucrose (612 mCi/mmol) and [^{3}H]water were purchased from Amersham International plc. The following cyclic nucleotides were purchased from Biolog Life Science Institute: *rp*-cAMPS, *sp*-cAMPS, 2-*aza*-ϵ-cAMP, 8-Br-cAMP, and 8-Cl-cAMP. The following cyclic nucleotides were purchased from the Sigma Chemical Co.: cAMP, N^6,2′-*O*-dibutyryl-3′,5′-cAMP, N^6-monobutyryl-cAMP, and N^6,2′-*O*-dibutyryl-3′,5′-cGMP. All other chemicals were of the best available grade.

Liver Perfusion

Male albino rats (Wistar), weighing 180–220 g, were fed *ad lib*. with a standard laboratory diet (Purina®). For the surgical procedure, the rats were anesthetized by i.p. injection of sodium pentobarbital (50 mg/kg). Hemoglobin-free, non-recirculating perfusion was performed. The surgical technique was that described by Scholz and Bücher [14]. After cannulation of the portal vein and vena cava, the liver was positioned in a plexiglass chamber. The flow was maintained constant by a peristaltic pump. The perfusion fluid was Krebs–Henseleit–bicarbonate buffer (pH 7.4), saturated with a mixture of oxygen and carbon dioxide (95:5) by means of a membrane oxygenator with simultaneous temperature adjustment at 37°.

Multiple-Indicator Dilution Experiments

Multiple-indicator dilution experiments [7, 10] were done by injecting into the portal vein 250 μL of a mixture containing [^{14}C]sucrose (5 μCi), [^{3}H]water (20 μCi), and one of the following cyclic nucleotides: [^{32}P]cAMP (2.5 μCi), [^{3}H]N^6,2′-*O*-dibutyryl-cAMP (5 μCi), *sp*-cAMPS (1 μmol), *rp*-cAMPS (1 μmol), 8-Cl-cAMP (1 μmol), 8-Br-cAMP (1 μmol), N^6-monobutyryl-cAMP (1 μmol), 2-*aza*-ϵ-cAMP (1 μmol), or N^6,2′-*O*-dibutyryl-cGMP (1 μmol). The effluent perfusate was collected in 0.5- to 2.0-sec fractions over a period of 90 sec following injection by means of a specially designed fraction collector [7, 10]. Radioactivity was measured by liquid scintillation. The scintillation solution contained toluol:ethanol (10:2) and 5.0 g/L of 1,5-diphenyloxazole plus 0.2 g/L of 2,2-*p*-phenyl-bis-5-phenyleneoxazole. When [^{14}C]sucrose, [^{3}H]water, and [^{32}P]cAMP were present simultaneously, they were distinguished by triple isotope discrimination. Samples containing [^{14}C]sucrose, [^{3}H]water, and [^{3}H]N^6,2′-*O*-dibutyryl-cAMP were divided into two aliquots. The first one was used for ^{14}C and total ^{3}H determination by means of isotope discrimination. [^{3}H]Water was removed from the second aliquot by freeze-drying. This procedure allowed the determination of [^{3}H]N^6,2′-*O*-dibutyryl-cAMP. Tritiated water in these samples was calculated as the difference between total counts and counts remaining after freeze-drying. Samples containing [^{14}C]sucrose, [^{3}H]water, and non-radioactive cyclic nucleotides were also divided into two aliquots. One of these aliquots was used for radioactivity determination, and the other one was diluted for spectrophotometric determination of the cyclic nucleotide in the ultraviolet range (250–275 nm, depending on the specific substance). The total injected amount of each cyclic nucleotide was calculated as (cyclic nucleotide/[^{14}C]sucrose) injected × ([^{14}C]sucrose recovered). This is justified by the fact that the recovery of labeled sucrose is complete [7, 15]. All dilution curves were normalized according to the relation (amount in the effluent sample × sec^{-1} × total amount $injected^{-1}$).

Search for Products Resulting from [^{32}P]cAMP and [^{3}H]N^{6}-2′-O-Dibutyryl-cAMP

The possible presence of [^{32}P]phosphate and [^{32}P]AMP as products of [^{32}P]cAMP transformation in the extracellular space was assessed by means of a technique that leads to specific precipitation of these compounds by nascently formed $Zn(OH)_2 \cdot BaSO_4$ [8]. Nascent $Zn(OH)_2 \cdot BaSO_4$ was formed by the addition of 0.1 vol. of aqueous 0.5 M $ZnSO_4$ followed by 0.1 vol. of 0.5 M $Ba(OH)_2$ to perfusate samples. The precipitate was compacted by centrifugation, and the entire procedure was repeated once more. The radioactivity remaining in the final supernatant was counted. Controls showed that the precipitation of phosphate and AMP was complete. The recovery of cAMP, which was determined by running appropriate controls, was around 60%. The possible presence of metabolic products of [^{3}H]N^{6},2′-*O*-dibutyryl-cAMP in the perfusate was investigated by means of HPLC using a Shim-Pack (CLC-ODS) 15-cm column (Shimadzu). Elution was started with aqueous 0.044 mM KH_2PO_4 (pH 6.0), which was replaced gradually and linearly by aqueous 0.044 mM KH_2PO_4 (pH 7.0) + methanol (1:1). The total elution time was 50 min.

Model Analysis

The outflow profiles obtained in the multiple-indicator dilution experiments were analyzed employing the space-distributed variable transit time model proposed by Goresky and co-workers [6, 15]. For the hemoglobin-free perfused rat liver [7], the normalized outflow profile of a substance (Q[t]) that exchanges with the cellular space and is irreversibly sequestered can be described by a function of time (t) containing the transfer coefficients for influx (k_{in}) and efflux (k_{ef}) and the intracellular transformation coefficient (k_m):

$$Q(t) = Q_{ref}(t) \cdot e^{-(k_{in})(t - t_0)} + \int_0^{t - t_0} e^{-(k_{ef} + k_m)(t - t_0 - \tau)} e^{-(k_{in}\tau)} \times Q_{ref}(\tau + t_0) \sum_{n=1}^{\infty} \frac{(k_{in}k_{ef}\tau)^n (t - t_0 - \tau)^{n-1}}{n!(n-1)!} d\tau \quad (1)$$

$Q_{ref}(t)$ is the normalized outflow profile of a substance that undergoes flow-limited distribution into the same extracellular space as the substance being investigated and that has no access to the cellular space; this curve represents the heterogeneity of the microcirculatory pathways (τ). The symbol t_0 stands for the uniform transit time in the large vessels. In equation (1), the dimensions of k_{in} are mL × (sec)$^{-1}$ × (mL accessible extracellular space)$^{-1}$; the dimensions of k_{ef} and k_m are mL × (sec)$^{-1}$ × (mL accessible intracellular space)$^{-1}$.

In the present work the extracellular reference curves ($Q_{ref}(t)$) were generated from the experimental [^{14}C]sucrose outflow profiles by means of the following linear transformation [15]:

$$Q_{ref}(t) = \left[\frac{1}{1 + \beta}\right] Q_{suc}\left(\frac{t - t_0}{1 + \beta} + t_0\right) \quad (2)$$

According to equation (2), the reference curve $Q_{ref}(t)$ is equal to the outflow profile of labeled sucrose at time $[(t - t_0)/(1 + \beta) + t_0]$ and divided by the factor $(1 + \beta)$. The parameter β is the excess extracellular space into which the cyclic nucleotide undergoes flow-limited distribution divided by the sucrose space. Equation (2) is analogous to the relation that exists between the labeled sucrose and tritiated water outflow profiles, i.e.

$$Q_{water}(t) = \left[\frac{1}{1 + \theta}\right] Q_{suc}\left(\frac{t - t_0}{1 + \theta} + t_0\right) \quad (3)$$

where θ is the ratio of intra- to extracellular spaces.

Equation (1) can be simplified considerably when the amount of material that returns to the extracellular space after permeation of the cell membrane is not significant, i.e. when $k_m \gg k_{ef}$. In this case, equation (1) reduces to

$$Q(t) = Q_{ref}(t) \cdot e^{-(k_{in})(t - t_0)} \quad (4)$$

Calculations

The first step in the model analysis of each experiment was the determination of the transit time in the large vessels (t_0) and the ratio of intracellular to extracellular water spaces (θ). These parameters were obtained in an optimized superposition of the normalized outflow profile of [^{3}H]water on the outflow profile of [^{14}C]sucrose, as predicted by equation (3). A nonlinear iterative least-squares procedure was used [16]. In the next step, equations (1) and (2) or (4) and (2) were fitted simultaneously to the experimental outflow profile of the cyclic nucleotide, using the optimized t_0 value together with preliminary estimates of k_{in}, k_{ef}, k_m, and β. Iteration was continued until the residual mean squares were minimized. Interpolation between experimental points, which is necessary when calculating equations (1), (2), and (3), was accomplished by means of a spline function [17]. The integral in equation (1) was calculated by means of Romberg's algorithm [17]. The time integrals ($\int_0^\infty Q(t)dt$) and the mean transit times ($\bar{t} = \int_0^\infty t \cdot Q(t)dt$; [18]) were determined by means of the trapezoid rule with monoexponential extrapolation to infinity [7, 8].

Rates of influx (F_{in}), net metabolic transformation (F_{met}), and the intracellular dibutyryl-cAMP concentrations were calculated from the transfer and transformation coefficients and the extracellular concentrations as follows [19, 20]:

$$F_{in} = (k_{in}/\theta)C_e \quad (5)$$

$$F_{met} = \frac{k_{in}k_m/\theta}{k_{ef} + k_m} C_e \quad (6)$$

$$C_i = \frac{k_{in}/\theta}{k_{ef} + k_m} C_e \quad (7)$$

Equations (5), (6), and (7) were derived by assuming steady-state conditions [19, 20]. C_e represents the extracellular non-tracer concentration, and θ represents the ratio of intra- to extracellular spaces. The introduction of this factor allows one to refer both F_{in} and F_{met} to the intracellular space. C_e is the logarithmic mean concentration along the sinusoidal beds, calculated from the portal and venous concentrations as proposed by Goresky *et al.* [21].

Fitting of the Michaelis–Menten equation to the N^6,2′-*O*-dibutyryl-cAMP influx data was performed by means of a nonlinear least-squares procedure using the Scientist® program [16]. The same program was used for linear regression analysis.

RESULTS

Outflow Profiles of Cyclic Nucleotides

Typical outflow profiles of cyclic nucleotides and references are shown in Figs. 1 and 2. The graphs in these figures are representative of the behaviour of the cyclic nucleotides utilized in the present study. In those experiments in which radioactive tracers were injected (Fig. 1), the injection was preceded by a 15-min infusion of the non-labeled analog. Figure 1A shows the dilution curves of [^{32}P]cAMP and the references [^{14}C]sucrose and [^{3}H]water. The non-tracer cAMP concentration was 50 μM. The [^{14}C]sucrose curve is the reference for the extracellular space and an indicator for the frequency distribution of the sinusoidal transit times. The [^{3}H]water curve is an indicator for the whole aqueous space of the liver. All curves were normalized by dividing the effluent radioactivity per unit time by the total injected radioactivity. Then the normalized data points were plotted against the time after injection. Data points obtained up to 35 sec are shown; however, all samples collected by the rapid sampling apparatus (up to 90 sec) were evaluated. The [^{32}P]cAMP data points in Fig. 1A are those measured after specific precipitation of [^{32}P]phosphate and [^{32}P]AMP by nascently formed $Zn(OH)_2 \cdot BaSO_4$ [8]. However, in all experiments, it was impossible to distinguish these data points from those obtained without precipitation of the putative products [^{32}P]phosphate and [^{32}P]AMP. Quantitatively, this is revealed by the single-pass recovery of the injected [^{32}P]cAMP radioactivity, which was equal to 0.944 ± 0.0144 (N = 12) in the untreated samples and 0.932 ± 0.0093 in the samples treated with nascently formed $Zn(OH)_2 \cdot BaSO_4$. The recovery was calculated as the area under the dilution curve, with monoexponential extrapolation to infinity ($\int_0^\infty Q(t)dt$). These results indicate that the formation of [^{32}P]phosphate and [^{32}P]AMP during a single passage through the liver was minimal, and the difference between the outflow profiles of [^{32}P]cAMP and [^{14}C]sucrose was likely to reflect predominantly uptake into the cell space. The difference between the [^{32}P]cAMP and [^{14}C]sucrose curves was small for all non-tracer cAMP concentrations between 10 and 100 μM, but reproducible.

The outflow profile of [^{3}H]dibutyryl-cAMP shown in Fig. 1B was also obtained with a non-tracer dibutyryl-cAMP concentration of 50 μM. The presence of metabolites of [^{3}H]dibutyryl-cAMP in the outflowing perfusate was assessed by HPLC at various times after the injection (see Materials and Methods). Besides the impurities normally present in the preparation (2–3%), no metabolic products were found in the perfusate. The [^{3}H]dibutyryl-cAMP curve differed markedly from the extracellular reference curve. The peak value was considerably lower, and the whole curve remained within the envelope of the reference curve. The difference between the [^{3}H]dibutyryl-cAMP and reference curves decreased when the non-tracer concentrations were increased, but the main characteristics shown by the graph in Fig. 1B were maintained. The single-pass recovery of [^{3}H]dibutyryl-cAMP varied between 0.6 and 0.8, revealing a much higher net uptake when compared with cAMP.

Figure 2 shows two typical outflow profiles of cyclic nucleotides that were injected in non-radioactive form and measured spectrophotometrically. In all cases, a quantity as close as possible to 1 μmol was injected. It is difficult to measure the recovery of the non-radioactive cyclic nucleotides very accurately because the absorbance of the samples in the tail portion is very low and can hardly be distinguished from the blank values. However, the injected amount can be determined with the same accuracy as that of the radioactive analogs, so that the normalization is correct. The normalized *rp*-cAMPS curve, shown in Fig. 2A, reveals a smaller peak value than the [^{14}C]sucrose curve. Actually, the *rp*-cAMPS curve ran below the reference curve until approximately 12.5 sec after injection. After this time, the *rp*-cAMPS tended to remain above the reference curve. Among all other cyclic nucleotides used in this work, only *sp*-cAMPS presented the same behaviour (data not shown). This probably is due to the fact that the *rp*- and *sp*-adenosine-3′,5′-cyclic monophosphorothioates are not metabolized in the liver, and the tail portion reflects material returning from the cell space. All other cyclic nucleotides injected in non-radioactive form behaved similarly to dibutyryl-cGMP, as illustrated by Fig. 2B. These cyclic nucleotides were 8-Cl-cAMP, 8-Br-cAMP, N^6-monobutyryl-cAMP, and 2-*aza*-ϵ-cAMP. The dibutyryl-cGMP curve in Fig. 2B was similar to the [^{3}H]dibutyryl-cAMP curve in Fig. 1B in that it remained within the envelope of the reference curve. However, the dibutyryl-cGMP outflow profile was much closer to the extracellular reference curve.

Model Analysis of the [^{32}P]cAMP Outflow Profiles

Model analysis should allow the calculation of transport parameters. For this purpose, we have tried to fit equations (1) and (2) or (4) and (2) to all outflow profiles obtained in the present work. The first step was to obtain the transit time in the large vessels (t_0) by means of an optimized

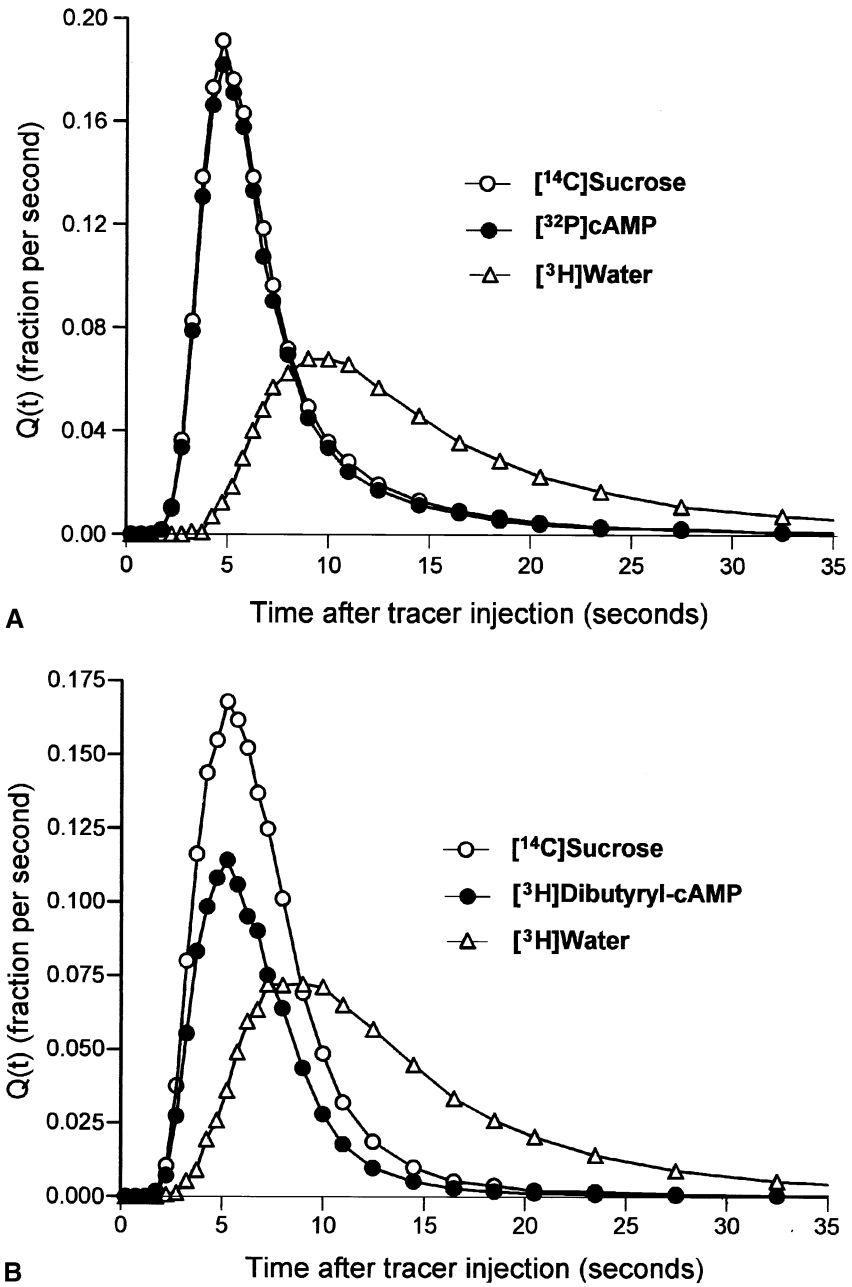

FIG. 1. Typical outflow profiles of [^{32}P]cAMP and [^{3}H]N^{6},2′-O-dibutyryl-cAMP plus indicators. Livers were perfused as described in Materials and Methods. cAMP or N^{6},2′-O-dibutyryl-cAMP was infused in separate perfusion experiments at concentrations equal to 50 μM. After 15 min, tracer amounts of [^{32}P]cAMP (≈2 μCi) plus indicators (A) or [^{3}H]N^{6},2′-O-dibutyryl-cAMP (≈5 μCi) plus indicators (B) were injected rapidly into the portal vein. The effluent perfusate was sampled, and the radioactivity in each sample was expressed as a fraction of the injected amount per second (Q(t)). The curves in panels (A) and (B) are representative of 3 and 4 indicator dilution experiments, respectively.

superposition of the [^{3}H]water and [^{14}C]sucrose curves according to equation (3). Then the value of t_0 was introduced into equations (1) and (2) or (4) and (2) together with provisional estimates of β and of the transfer and transformation coefficients k_{in}, k_{ef}, and k_m. Iterations of the nonlinear least-squares procedures were continued until the standard deviation of the estimate was minimized. In the case of the [^{32}P]cAMP curves, fitting of equations (1) and (2) was not possible. The calculations either produced negative values or, more frequently, the values of k_{ef} and k_m approached infinity without improvement of the standard deviation of the estimate. This means that the [^{32}P]cAMP outflow profiles did not present significant amounts of material returning from the cell space, i.e. $k_m \gg k_{ef}$. Equations (4) and (2), however, could be fitted to all [^{32}P]cAMP outflow profiles. An example is shown in Fig. 3A. The calculated curve matched the experimental one with perfection. As expected from the small difference

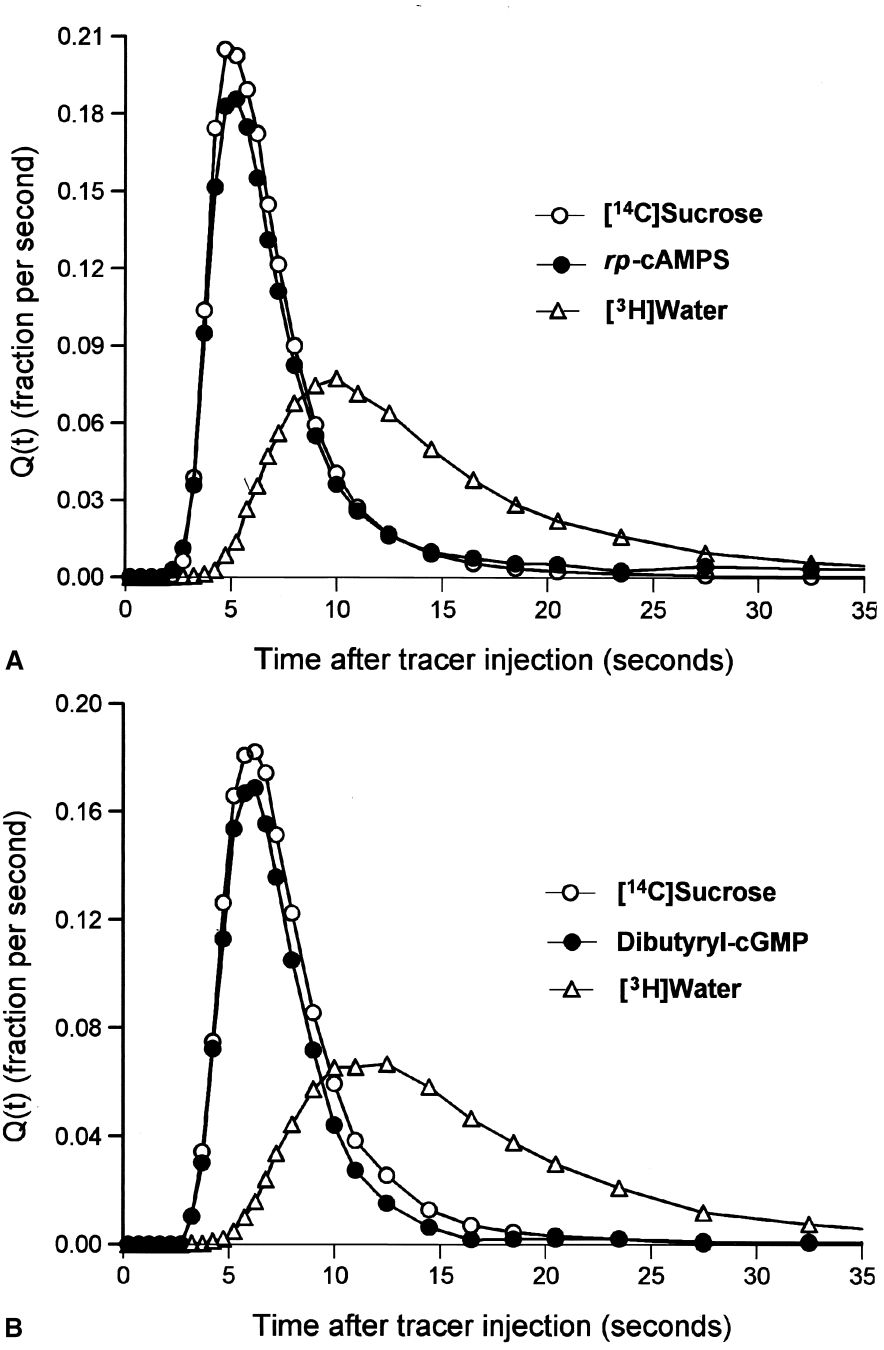

FIG. 2. Typical outflow profiles of *rp*-cAMPS and N^6,2′-*O*-dibutyryl-cGMP plus indicators. Livers were perfused as described in Materials and Methods. *rp*-cAMP (1 μmol) plus indicators (A) or N^6,2′-*O*-dibutyryl-cGMP (1 μmol) plus indicators (B) were injected rapidly into the portal vein. The effluent perfusate was sampled. *rp*-cAMPS and N^6,2′-*O*-dibutyryl-cGMP were measured spectrophotometrically; [^{14}C]sucrose and [^{3}H]water were determined by liquid scintillation counting. The quantity in each sample was expressed as a fraction of the injected amount per second (Q(t)). The curves in panels (A) and (B) are representative of 3 and 4 indicator dilution experiments, respectively.

between the [^{32}P]cAMP and [^{14}C]sucrose curves, the values of k_{in} were relatively low. No significant variation was observed in the various non-radiactive cAMP concentrations in the perfusion fluid, and the mean value was equal to 0.0143 ± 0.00097 mL sec^{-1} (mL extracellular space)$^{-1}$ or 0.86 ± 0.058 mL min^{-1} (mL extracellular space)$^{-1}$ (see Table 1). The value of β, on the other hand, was always small (mean value: 0.0135 ± 0.0019). From the definition of β in Materials and Methods, this means that the [^{14}C]sucrose curve is the appropriate reference for the cAMP outflow profiles.

If equation (4) is written in logarithmic form, it can be easily shown that $\ln [Q_{ref}(t)/Q(t)] = k_{in}(t - t_0)$. This means that $\ln [Q_{ref}(t)/Q(t)]$ should be a linear function of

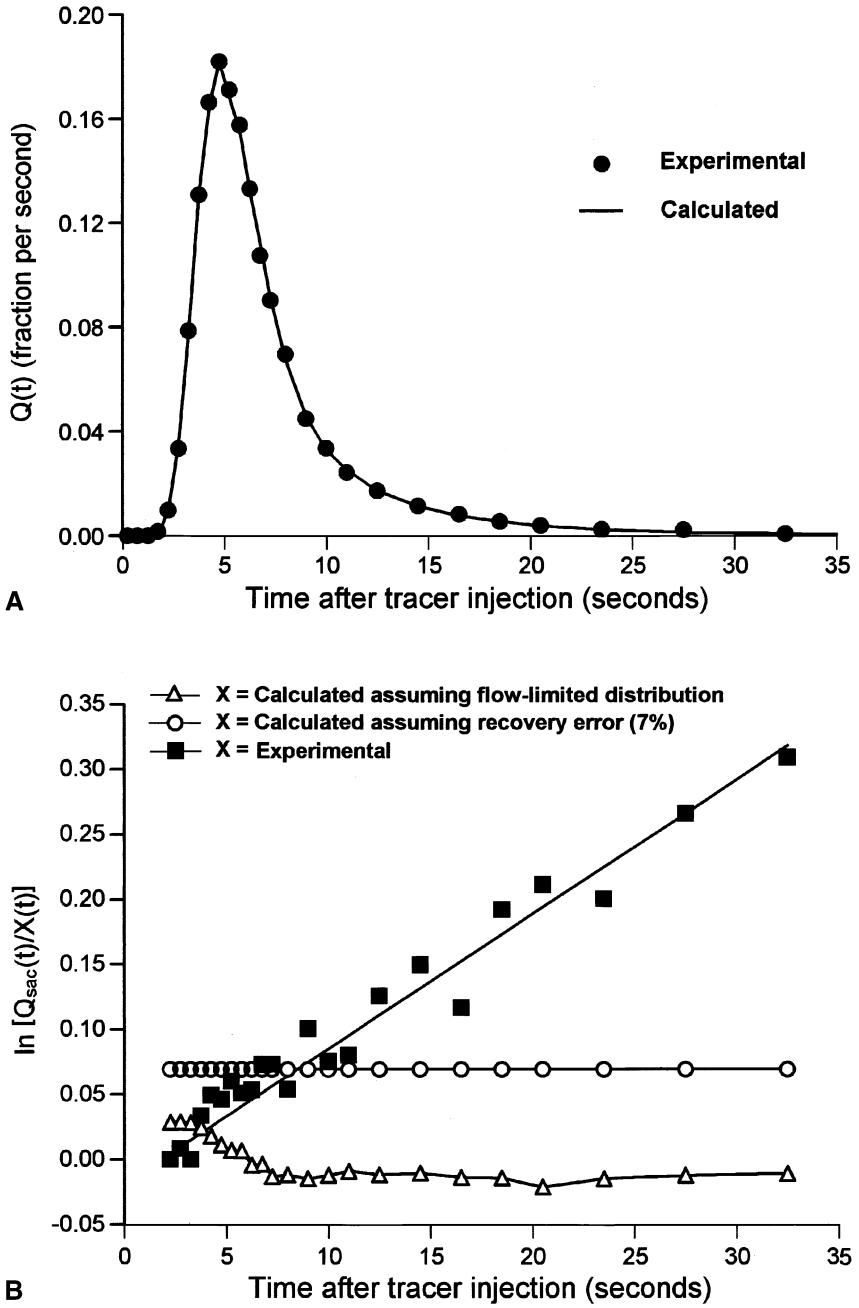

FIG. 3. Model analysis of a [^{32}P]cAMP outflow profile. Panel A shows an experimental [^{32}P]cAMP outflow profile and the theoretical curve obtained by fitting equation [1] to these data. The optimized parameters were: β = 0.0098; k_{in} = 0.0118 mL sec^{-1} (mL extracellular space)$^{-1}$; t_0 = 1.786 sec. In panel B, several logarithmic $Q_{sac}(t)/X$ ratios were plotted against time in which X was representing: (a) experimental [^{32}P]cAMP data; (b) a theoretical curve generated from the experimental [^{14}C]sucrose outflow profile by linear transformation according to equation [3] with a space ratio of 1.072 and t_0 = 1.786 sec; and (c) a theoretical curve generated from the experimental [^{14}C]sucrose outflow profile assuming an error of −7% in the recovery determination. $Q_{sac}(t)$ represents the outflow profile of [^{14}C]sucrose.

time, provided that equation (4) is really a good description for the [^{32}P]cAMP outflow profiles [6]. Figure 3B confirms this prediction, which actually was expected due to the agreement between the calculated and experimental curves in Fig. 3A. However, the type of representation in Fig. 3B allows us to exclude two possible sources of error in the interpretation of the [^{32}P]cAMP outflow profiles. The first one is a systematic error in the calculation of the recovery, and the second one is a very rapid, flow-limited distribution of cAMP into a space slightly greater than the sucrose space, but still on the outside of the cell. Figure 3B shows that the first possibility should produce a constant $Q_{ref}(t)/Q(t)$ ratio. The second possibility, on the other hand, is more likely to produce a complex curve that shows little

TABLE 1. Transfer coefficients of several cyclic nucleotides

Cyclic nucleotide	Influx (k_{in}) (mL min^{-1} mL extracellular $space^{-1}$)	Influx (k_{in}) k_{in} of cAMP = 1	Efflux (k_{ef}) (mL min^{-1} mL intracellular $space^{-1}$)	N
cAMP (10–100 μM)	0.860 ± 0.058	1.00		13
N^6-Monobutyryl-cAMP (1 μmol)	1.146 ± 0.222	1.33		4
2-*aza*-ϵ-cAMP (1 μmol)	1.152 ± 0.294	1.34		4
rp-cAMPS (1 μmol)	1.692 ± 0.048	1.97	1.190 ± 0.510	3
sp-cAMPS (1 μmol)	1.872 ± 0.432	2.18	1.044 ± 0.162	5
8-Br-cAMP (1 μmol)	2.064 ± 0.232	2.40		4
N^6,2′-*O*-Dibutyryl-cGMP (1 μmol)	2.142 ± 0.303	2.49		4
8-Cl-cAMP (1 μmol)	2.178 ± 0.372	2.53		3
N^6,2′-*O*-Dibutyryl-cAMP				
First order conditions	6.873 ± 0.796	7.99	5.596 ± 2.114	12
At half-saturating concentrations (calculated)	3.63	4.22		

The mean transfer coefficients obtained by fitting equations (1) and (2) or (4) and (2) to the experimental outflow profiles are listed with the corresponding SEM. The values for all cAMP analogs, except dibutyryl-cAMP, correspond to a bulk injection of 1 μmol, which generated mean sinusoidal concentrations within the range of 10 to 100 μM. First order conditions in the case of N^6,2′-*O*-dibutyryl-cAMP corresponds to the linear initial portion of the saturation curve shown in Fig. 5A. The value for half-saturating conditions was calculated as $V_{max}/(K_m + [C_e]_{1/2})$; $[Ce]_{1/2}$ is the dibutyryl-cAMP concentration for half-maximal saturation.

resemblance to a linear relationship. The latter curve was generated from a theoretical cAMP curve calculated according to equation (2) and assuming a space ratio (1 + β) equal to 1.07.

Model Analysis of the [^{3}H]Dibutyryl-cAMP Outflow Profiles

Contrary to the [^{32}P]cAMP curves, the [^{3}H]dibutyryl-cAMP outflow profiles contained sufficient returning material to allow the determination of k_{ef} and k_m in addition to k_{in} and β. This means that fitting of equations (1) and (2) to the [^{3}H]dibutyryl-cAMP curves was successful. An example is shown in Fig. 4. The values of k_{in} for [^{3}H]dibutyryl-cAMP were always higher than those obtained for [^{32}P]cAMP and varied considerably with the concentration of non-tracer dibutyryl-cAMP. The value of k_{ef} was, in general, smaller than k_m, but always of the same order of magnitude. This means that the metabolic transformation of dibutyryl-cAMP was limited by both transport and the enzymatic systems. Besides the experimental points and the

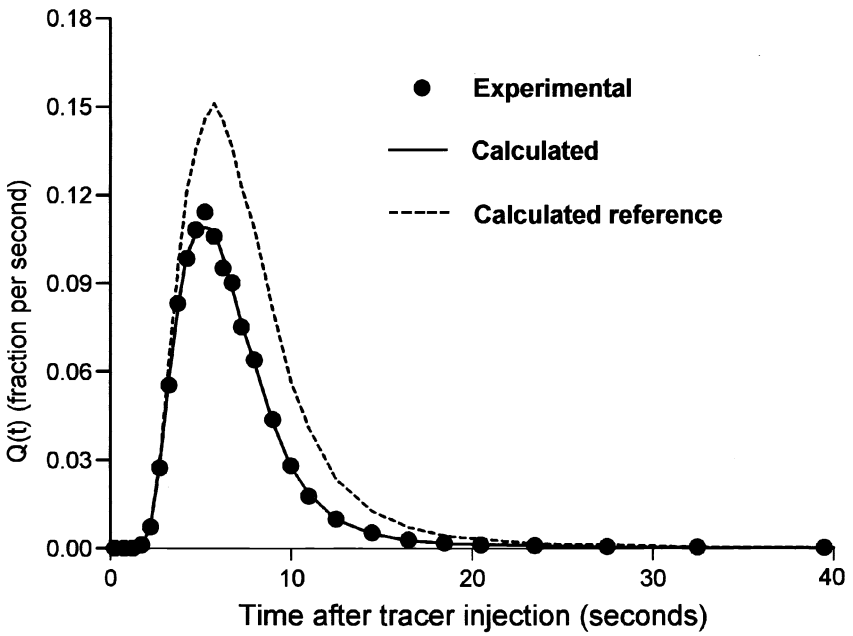

FIG. 4. Model analysis of a [^{3}H]dibutyryl-cAMP outflow profile. Equation [1] was fitted to the experimental outflow profile of [^{3}H]dibutyryl-cAMP shown in Fig. 1B. The theoretical outflow profile was calculated employing equation [1], with β = 0.10, k_{in} = 0.093 mL sec^{-1} (mL extracellular space)$^{-1}$, k_{ef} = 0.00507 mL sec^{-1} (mL cellular space)$^{-1}$, K_m = 0.0416 mL sec^{-1} (mL cellular space)$^{-1}$, and t_o = 2.086 sec. The reference curve was generated from the [^{14}C]sucrose outflow profile according to equation [2], with β = 0.10 and t_o = 2.086 sec.

calculated outflow profile, Fig. 4 also shows the computed reference ($Q_{ref}[t]$). In contrast to the cAMP experiments, the calculated reference curve for [^{3}H]dibutyryl-cAMP differed from the [^{14}C]sucrose outflow profile to an extent that could affect the determination of k_{in}, k_{ef}, and k_m appreciably. The β value was equal to 0.11 in the experiment shown in Fig. 4, but it varied between 0.02 and 0.15. Apparently the extracellular space into which dibutyryl-cAMP underwent flow-limited distribution is somewhat greater than that of cAMP.

Concentration Dependence of cAMP and Dibutyryl-cAMP Transport and Metabolism

Using equations (5) and (6), the rates of influx of cAMP and dibutyryl-cAMP and the rates of net transformation of dibutyryl-cAMP were calculated and plotted against the extracellular concentration, as shown in Fig. 5. Influx and net transformation of dibutyryl-cAMP were both saturable functions of the extracellular concentration. The difference between the net transformation and influx rates corresponds to the efflux rates, which were considerably lower than the influx rates. The well known Michaelis–Menten equation ($F_{in} = V_{max} \cdot C_e/[K_m + C_e]$) was fitted to the F_{in} versus C_e data in Fig. 5A. The line joining the experimental data was calculated with the fitted parameters K_m and V_{max}. The Michaelis–Menten equation accounted very well for the experimental curve. The K_m value, which corresponds to the concentration for half-maximal influx rate, was equal to 72.75 ± 9.24 μM. The maximal rate (V_{max}) was 0.464 ± 0.026 μmol min^{-1} (mL cellular space)$^{-1}$.

The rate of influx of cAMP did not show an obvious saturation for extracellular concentrations up to 100 μM, as revealed by Fig. 5B. Strictly speaking, the points describe a curve with a very slight curvature. This is a consequence of the fact that the k_{in} values showed little change when the perfusate cAMP concentration was varied. Since for cAMP $k_m \gg k_{ef}$, intracellular metabolic transformation of cAMP is limited predominantly by the rate of permeation. This means that for cAMP the values of F_{met} should be practically equal to those of F_{in}. Comparison of the ordinate scales of panels A and B in Fig. 5 reveals that dibutyryl-cAMP permeated the cell membrane at rates that were several times higher than those at which cAMP entered the cell. For a portal cAMP concentration of 100 μM, the influx rate was equal to 47 μmol min^{-1} (mL cell space)$^{-1}$. With dibutyryl-cAMP, a comparable rate can be expected at a concentration of 8 μM.

For cAMP, $k_m \gg k_{ef}$ as already stated above. From equation (7) in Materials and Methods, it follows that the intracellular concentration of this compound must be very low when compared with the extracellular concentration. Even in the case of dibutyryl-cAMP the intracellular concentration was considerably lower than the extracellular concentration, especially when the latter was below 50 μM as revealed by panel A in Fig. 6. In this panel, the C_i/C_e ratios were plotted against C_e. The calculated C_i values (and by extension also the C_i/C_e values) showed a considerable dispersion. This is due to the fact that the correlation between k_{ef} and k_m when fitting equations (1) and (2) to the experimental data was relatively pronounced. This has the consequence that although the ratio $k_m/(k_{ef} + k_m)$ can still be determined with confidence [equation (6)], the determination of the sum $k_{ef} + k_m$ [equation (7)] is much more subject to error. Even so, it can be recognized that C_i/C_e increased when C_e increased. This observation can be attributed to a saturation of the intracellular removal process or processes. The saturation of F_{met} versus C_e shown in Fig. 5A represents, thus, the superposition of two saturation processes, influx and metabolic transformation.

Panel B in Fig. 6 shows the mean transit times of [^{3}H]water, [^{14}C]sucrose, and of the computed reference for dibutyryl-cAMP, plotted against the portal dibutyryl-cAMP concentration. The first two parameters did not vary with dibutyryl-cAMP up to 200 μM. This means also that the hemodynamics and the cellular and vascular spaces in the liver were not affected by dibutyryl-cAMP. The mean transit time of the computed reference showed a small tendency toward decreasing values as the dibutyryl-cAMP concentration was raised.

Influence of cAMP on Dibutyryl-cAMP Transport and on Hemodynamics

The saturable relation between dibutyryl-cAMP influx and perfusate concentration suggests that the entry of that substance into the cell does not occur by simple diffusion and, consequently, depends on specific binding. If this is true, one can expect competition and inhibition of transport by substances with similar structural properties. For this reason, several experiments were done in which the transport of dibutyryl-cAMP was measured in the presence of cAMP. Labeled substances were injected 15 min after starting the simultaneous infusion of cAMP and dibutyryl-cAMP. The dibutyryl-cAMP concentration was always 10 μM; that of cAMP varied between 0.2 and 2.0 mM. The mean results of these experiments are shown in Fig. 7. Panel A in Fig. 7 relates the dibutyryl-cAMP influx rates to the cAMP concentration. cAMP inhibited dibutyryl-cAMP transport; 50% inhibition, as determined by means of numerical interpolation, occurred at a cAMP concentration of 0.83 mM.

The concentrations of cAMP producing inhibition of dibutyryl-cAMP transport are relatively high, and they could be the consequence of changes in the hemodynamics or in the accessible cell spaces. For these reasons it is worthwhile to look at panel B in Fig. 7, where the mean transit times of labeled water, labeled sucrose, and of the computed reference for dibutyryl-cAMP were plotted against the cAMP concentration. As shown, no significant changes were detected with cAMP in the range up to 2.0 mM.

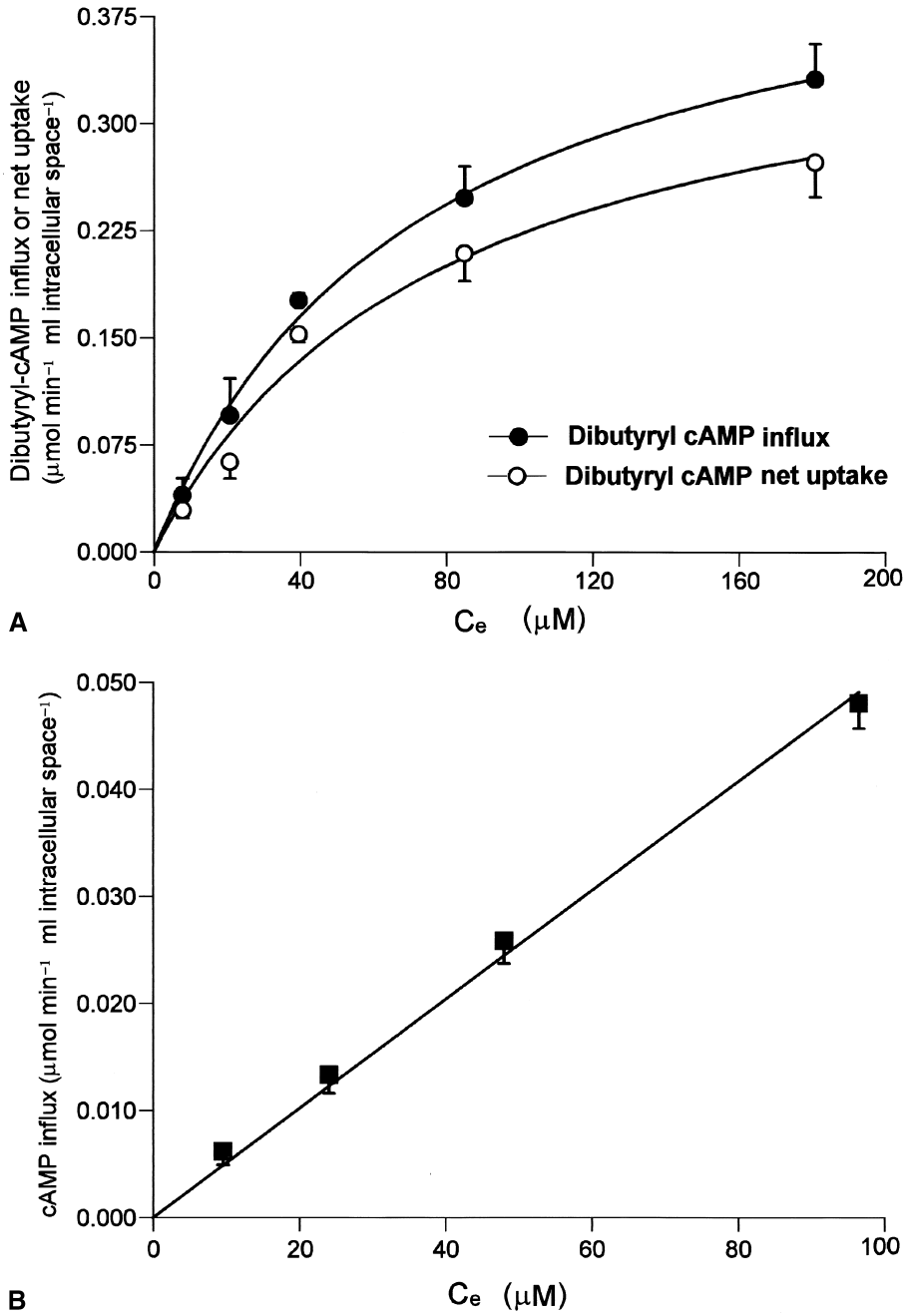

FIG. 5. Rates of unidirectional influx and net uptake as a function of the mean extracellular concentration (C_e). Panel A refers to N^6,2′-*O*-dibutyryl-cAMP and panel B to cAMP. The rates of unidirectional influx were calculated according to equation [5], using the rate constants derived by fitting equations [1] or [4] to the outflow profiles; the net uptake rates of N^6,2′-*O*-dibutyryl-cAMP were calculated employing equation [6]. C_e was calculated as a logarithmic mean according to Goresky *et al.* [21]. Each experimental point represents the mean of 3–5 indicator dilution experiments. Bars represent SEM. The continuous line joining the experimental influx rates of N^6,2′-*O*-dibutyryl-cAMP represents the optimized Michaelis–Menten curve, with V_{max} = 0.464 ± 0.026 μmol min^{-1} (mL cellular space)$^{-1}$ and K_m = 72.75 ± 9.24 μM.

Permeation Rates and Lipophilicity of the Various cAMP Analogs

The dilution curves resulting from the injection of the non-radioactive cAMP analogs and [^{3}H]water plus [^{14}C]sucrose (see Fig. 2 for examples) were also analyzed by means of equations (1) and (2) or (4) and (2). As expected from the form of their tail portions, the complete equations (1) and (2) could be fitted successfully to the outflow profiles of *rp*-cAMPS and *sp*-cAMPS. In this case, the transformation coefficient k_m was equated to zero, because it is known that these analogs are not transformed in mammalian cells [22]. For these analogs, thus, it was possible to obtain both k_{in} and k_{ef}. For all other analogs only k_{in} could be obtained because no sufficient information about returning material

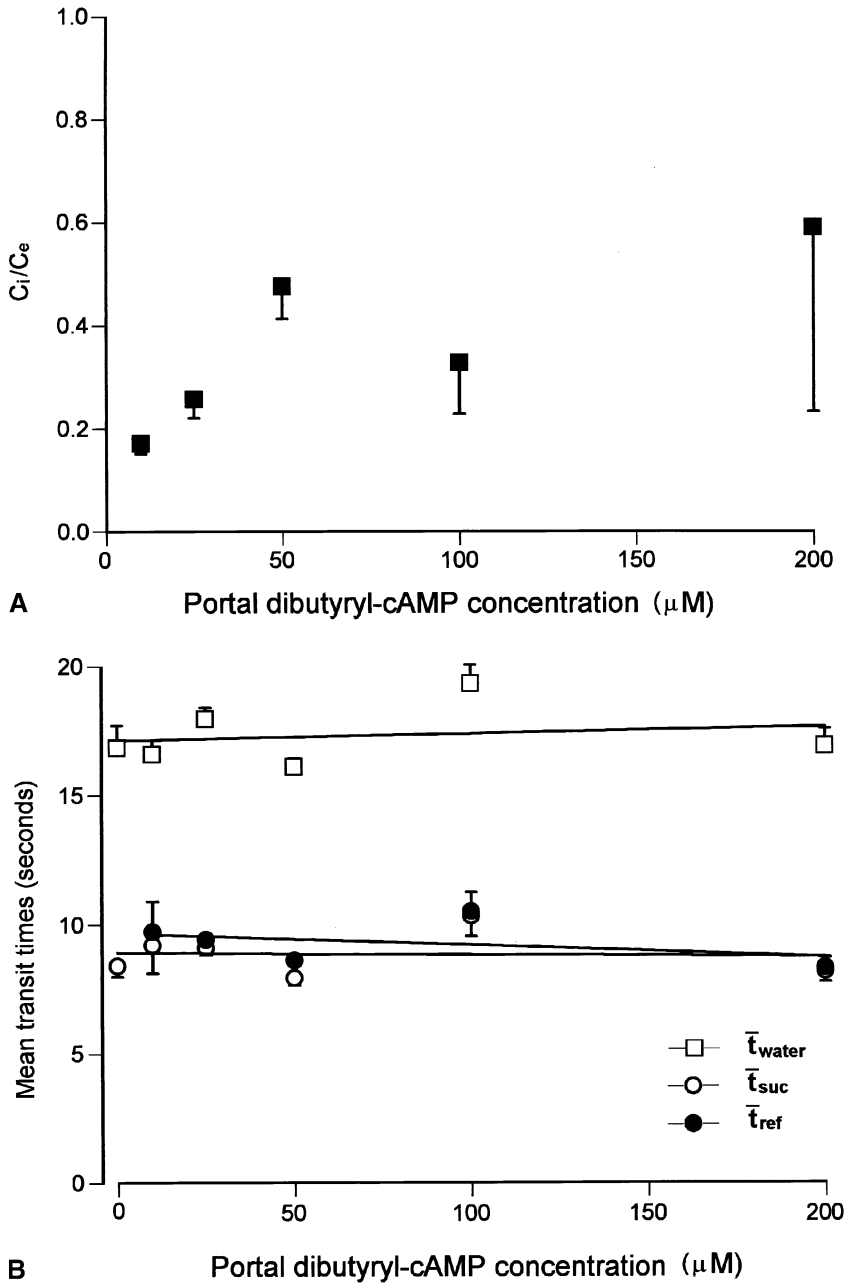

FIG. 6. Ratio of intra- to extracellular concentrations (C_i/C_e; panel A) and hemodynamic parameters (panel B) as a function of the portal dibutyryl-cAMP concentration. The C_i/C_e ratios were calculated from the rate constants according to equation [7]. The mean transit times were calculated by numerical integration. The data points are the means of 3–5 liver perfusion experiments. Bars represent SEM. The straight lines in panel B are the linear regression lines. The correlation coefficients for the $\bar{t}_{water}$, $\bar{t}_{suc}$, and $\bar{t}_{ref}$ curves are 0.17, 0.063, and 0.4, respectively.

was apparent in the outflow profiles. Table 1 lists the mean values of all transfer coefficients obtained in the present work. In those experiments in which the non-radioactive analogs were employed, the injected amount was always 1 μmol. The mean sinusoidal concentration generated by these concentrations was well within the range of the cAMP concentrations in those experiments in which [^{32}P]cAMP was injected (10–100 μM), without significant changes in the transfer coefficients, as revealed by the virtual absence of saturation (Fig. 5B). Comparison of the transfer coefficients obtained with [^{3}H]dibutyryl-cAMP with those of the non-radioactive analogs is less straightforward because transport of [^{3}H]dibutyryl-cAMP presents saturation (Fig. 5A). For this reason Table 1 presents values for the first order condition (i.e. the initial linear portion of the saturation curve in Fig. 5A) and values that are valid for half-saturating conditions. The latter are close to the conditions of the bulk injection of the non-radioactive analogs and should, thus, be preferred for comparative purposes. The sequence in which the compounds are listed

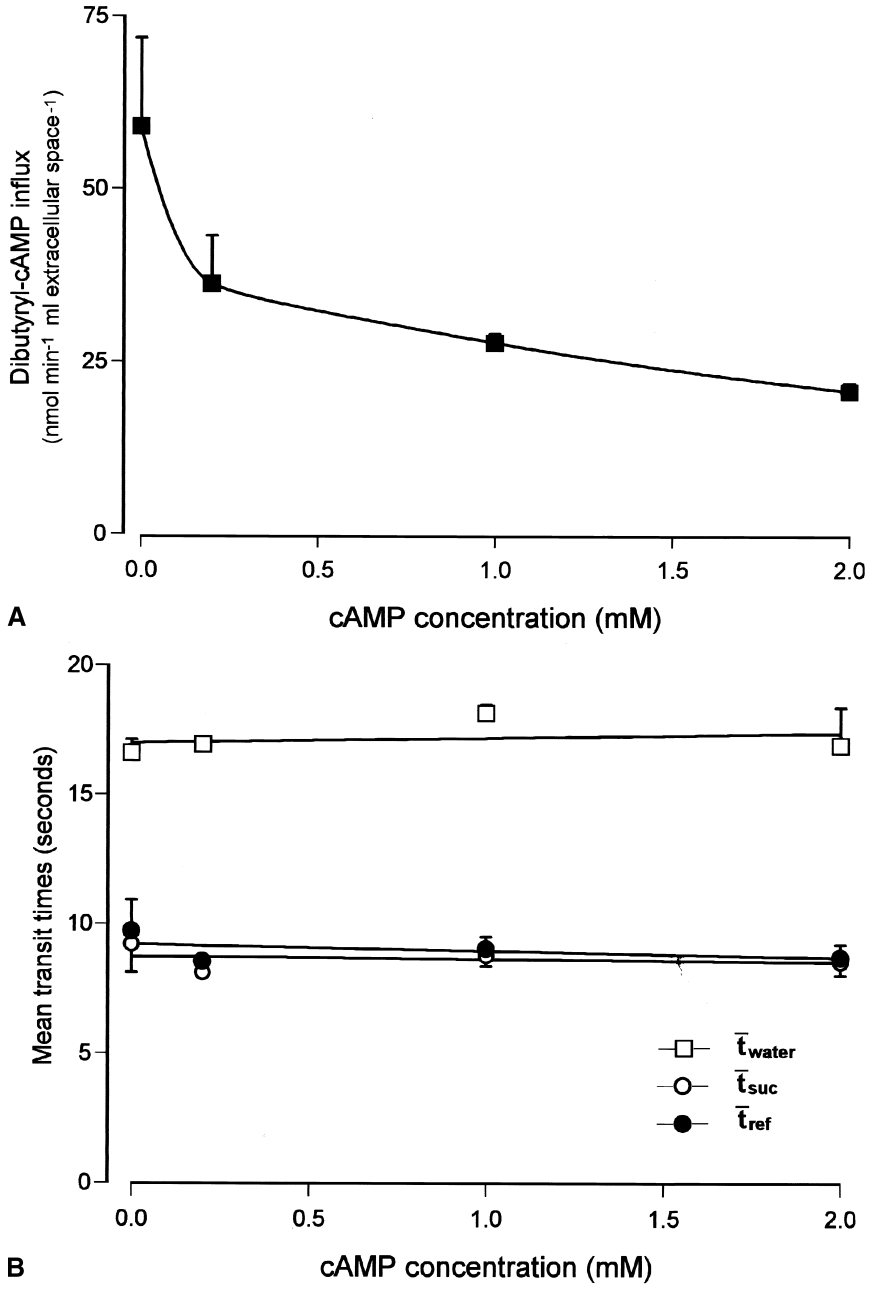

FIG. 7. Influence of cAMP on dibutyryl-cAMP influx (panel A) and on hemodynamic parameters (panel B). Rates of dibutyryl-cAMP influx were calculated according to equation [5], using the rate constants derived by fitting equations [1] and [2] to the outflow profiles. The mean transit times were calculated by numerical integration. Each data point represents the mean of three indicator dilution experiments. Bars represent SEM. The straight lines in panel B are the linear regression lines. The correlation coefficients for the $\bar{t}_{water}$, $\bar{t}_{suc}$, and $\bar{t}_{ref}$ curves are 0.25, 0.22, and 0.46, respectively.

in Table 1 follows the increasing values of k_{in}. cAMP has the lowest transfer coefficient and dibutyryl-cAMP the highest, even if one considers half-saturating conditions. The transfer coefficients for efflux, in those cases in which they could be measured, revealed values of the same order as that of influx.

A question that arises at this point is whether the transfer coefficient for influx correlates with the lipophilicity of the various analogs listed in Table 1. An answer to this question can be obtained from a graph of the k_{in} values against the corresponding lipophilicities, which can be obtained from the work of Krass *et al.* [23]. The indicator for lipophilicity used by those authors was actually the partition coefficient (K_w) of the substance between methanol and water. The result of this analysis is shown in Fig. 8. The figure reveals that the correlation between the transfer coefficients of the various cyclic nucleotides and their corresponding lipophilicity is relatively weak. The linear

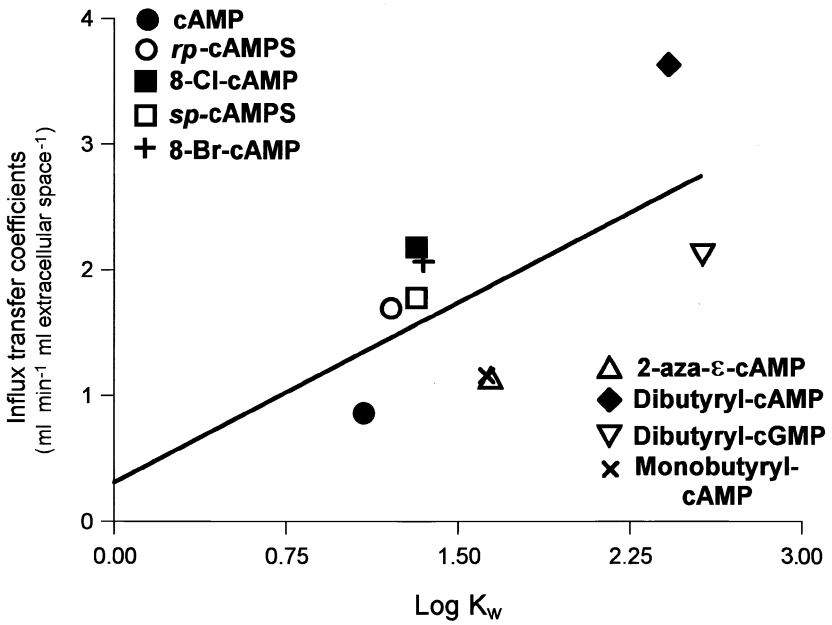

FIG. 8. Influx rate constants of cAMP and analogs as a function of the methanol:water partition coefficient (K_w). The influx rate constants listed in Table 1 were plotted against the partition coefficients reported by Krass *et al.* [23]. The continuous line represents the regression line, calculated as $\hat{y} = 0.952x + 0.308$; the correlation coefficient is 0.611 ± 0.216.

correlation coefficient obtained by regression analysis was equal to 0.611 ± 0.216. The individual discrepancies can be regarded as highly significant. For example, N^6-monobutyryl-cAMP is 3.5 times more lipophilic than cAMP; influx of N^6-monobutyryl-cAMP, however, was only 1.33 times faster. N^6,2′-*O*-Dibutyryl-cGMP is 17.4 times more lipophilic than 8-Br-cAMP, but their rates of influx were practically the same.

DISCUSSION

It seems likely that the transport of cAMP and its analogs in the liver is not a simple diffusion process. Three observations of the present work support this conclusion: (a) the transport of dibutyryl-cAMP into the cell was a saturable function of its concentration; (b) the transport of dibutyryl-cAMP was inhibited by cAMP, a substance that is similar in structure; and (c) the correlation between influx and lipophilicity of several cAMP analogs was relatively weak. If lipophilicity were the most important factor determining the movement across the cell membrane, a more unequivocal correlation between influx and lipophilicity should be observed. The discrepancies between lipophilicity and influx rates, in addition to the saturation and inhibition phenomena, are much more indicative of a facilitated transport mechanism. In this transport mechanism lipophilicity plays some role, but other group specificities seem to be equally effective in determining the penetration rates. The existence of facilitated transport for cAMP and analogs was also suggested by Holman [1] in human erythrocytes and by Coulson *et al.* [22] in the isolated perfused rat kidney. The evidence presented by Holman [1] consists of saturation kinetics, trans-effects, and inhibition by cytochalasin B. Coulson *et al.* [22] found inhibition of transport by the drug probenecid and lack of correlation between penetration rates and lipophilicity.

Although no clear saturation was found for cAMP influx, this should not be regarded as an indication that cAMP and dibutyryl-cAMP have different permeation mechanisms. Actually, the very slight tendency toward a concave-down curvature of the influx versus cAMP concentration dependence (Fig. 5B) is also consistent with a high K_m value. The concentration of cAMP that produced 50% inhibition of dibutyryl-cAMP transport was very high indeed (0.83 mM), and it is reasonable to expect that the K_m for cAMP influx is of the same magnitude or even larger.

In spite of the reports that cAMP can be hydrolyzed both intra- and extracellularly [24, 25], the single-pass extracellular hydrolysis was minimal in our experiments, as revealed by the absence of hydrolysis products in the outflowing perfusate. The intracellular transformation, however, is so fast as to avoid any significant return of labeled material to the extracellular space. Transport of exogenous cAMP, thus, is limiting intracellular transformation in such a way that high extracellular concentrations are required to achieve metabolic effects comparable to those of glucagon and dibutyryl-cAMP. Kagimoto and Uyeda [3] found intracellular cAMP concentrations around 4.2 μM when the extracellular cAMP concentration was equal to 100 μM. This means a concentration gradient of approximately 24-fold. This is consistent with our results, because if the rate of efflux of labeled cAMP is 24 times smaller than the rate of influx, the return of label during a single passage cannot be detected. It should be mentioned that intracel-

lular transformation of cAMP is a fast process only in relative terms, i.e. when compared with the low influx rates. If the coefficients of metabolic transformation of cAMP were of the same magnitude as that of dibutyryl-cAMP, for example (see legend to Fig. 4), they would already exceed those of influx by a factor of 10 or more.

In the case of dibutyryl-cAMP, intracellular transformation is limited by both the intracellular enzymic system (or systems) and the transport system. This is revealed by the fact that, during a single passage, some of the material that entered the cell reappeared in the extracellular space, allowing the determination of both the transfer coefficient for efflux and the coefficient for intracellular transformation. Castagna *et al.* [12] have measured the intracellular distribution of radioactivity during recirculating perfusion with labeled dibutyryl-cAMP. Many labeled compounds appeared in the cellular space including AMP, ADP, ATP, N^6-monobutyryl-cAMP, N^6-monobutyryl-AMP, and 2′-*O*-monobutyryl-cAMP. These compounds, however, did not appear in significant amounts in the extracellular space [12], an observation confirmed by our measurements. From the multiplicity of intracellular products it can be deduced that the irreversible sequestration of dibutyryl-cAMP involves not only the phosphodiesterase activity but also two different deacylases [26]. For this reason the coefficient for intracellular transformation measured in the present work corresponds, most probably, to the sum of at least three irreversible transformation coefficients.

Influx of cAMP was measured in the present work under conditions where the intracellular cAMP production was minimal (absence of hormones) and the extracellular concentration was high. These conditions, in addition to the intracellular phosphodiesterase activity, ensured a net flux of the compound from the medium into the cell space. These rather convenient conditions made it possible to measure cAMP transport in the inward direction. In physiological terms, however, the relevant condition is one in which the intracellular production of cAMP is significant because of hormonal stimulation, and a net efflux of the compound occurs. The cAMP that is released into the circulation will be excreted by the kidney [22], so that in this respect the *in vivo* situation resembles the once-through perfused liver. A question that can be formulated is whether the transfer rates measured in the present work are compatible with the rates of net cAMP release when the liver operates under hormonal stimulation. One way of analyzing this question is to calculate the intracellular cAMP pool in the presence of hormones using the transport parameters determined in the present work and then to compare these values with the experimental determinations. If disagreement is very pronounced, it must be concluded that the transport system detected in the present work is not compatible with the net efflux rate of cAMP in the presence of hormones. The net flux through the cell membrane (F_{net}) is the difference between influx (F_{in}) and efflux (F_{ef}), i.e.

$$F_{net} = F_{in} - F_{ef} = (k_{in}/\theta)C_e - k_{ef}C_i \quad \therefore$$

$$C_i = \frac{(k_{in}/\theta)C_e - F_{net}}{k_{ef}} \quad (8)$$

C_e and C_i are the intra- and extracellular cAMP concentrations, respectively, and k_{in} and k_{ef} are the transfer coefficients for influx and efflux already defined in Materials and Methods. The parameter θ represents the ratio of intra- to extracellular spaces, and it was introduced for referring the influx rate to the cellular space. Its mean value in the present work was 1.55. For cAMP the value of k_{in} was determined (Table 1) but not that of k_{ef}. However, it seems reasonable to expect that the k_{ef}/k_{in} ratio for cAMP is not significantly different from that found for the analogs *rp*-cAMPS and *sp*-cAMPS (Table 1). The mean k_{ef}/k_{in} ratio for these analogs was 0.63, which leads to a k_{ef} value of 0.54 mL min^{-1} (mL cellular space)$^{-1}$ for cAMP. The maximal rate of cAMP release (F_{net}) with 10 nM glucagon found in our laboratory with the same perfusion system utilized in the present work [5] was -1.6 nmol min^{-1} (mL cellular space)$^{-1}$. For a flow of 30 mL/min and a mean liver weight of 10 g, this efflux rate produces an extracellular cAMP concentration of 0.27 nmol/mL. Substitution of all these values in equation (8) and calculation produce C_i equal to 3 nmol/mL (3 μM). This calculated C_i represents a kind of averaged mean of the concentrations of the various forms of cAMP, as for example free form, particulate form, and protein-bound [27]. Even so, the value of 3 nmol/mL agrees fairly well with the reported range of the intracellular cAMP concentration in liver cells under the stimulus of glucagon [3, 28–30]. The permeability of the cell membrane to cAMP measured in the present work, thus, is compatible with the rates of cAMP release by the liver. Furthermore, the calculations reveal a C_i/C_e ratio of 11.1, and it is evident from equation (8) that any increase in k_{ef} will produce lower intracellular cAMP concentrations. If k_{ef} for cAMP were in the range of the values found for dibutyryl-cAMP, for example (see Table 1), approximately 10-fold higher rates of cAMP formation would be required to achieve intracellular concentrations capable of a significant stimulation of protein kinase A. Thus, the low permeability of the cell membrane to cAMP facilitates the creation of a concentration gradient favouring the cell space when its synthesis is under hormonal stimulation.

This work was supported by grants from the Conselho Nacional de Desenvolvimento Científico e Tecnológico (CNPq), the Programa Nacional de Núcleos de Excelência (PRONEX), and the Coordenação de Aperfeiçoamento do Pessoal de Ensino Superior (CAPES).

References

1. Holman GD, Cyclic AMP transport in human erythrocyte ghosts. *Biochim Biophys Acta* **508:** 174–183, 1978.
2. Rindler MJ, Bashor MM, Spitzer N and Saier MH Jr, Regulation of adenosine 3′:5′-monophosphate efflux from animal cells. *J Biol Chem* **253:** 5431–5436, 1978.

3. Kagimoto T and Uyeda K, Regulation of rat liver phosphofructokinase by glucagon-induced phosphorylation. *Arch Biochem Biophys* **203:** 792–799, 1980.
4. Levine RA, Lewis SE, Shulman J and Washington A, Metabolism of cyclic adenosine 3′,5′-monophosphate-8-^{14}C by isolated, perfused rat liver. *J Biol Chem* **244:** 4017–4022, 1969.
5. Constantin J, Suzuki-Kemmelmeier F, Yamamoto NS and Bracht A, Production, uptake, and metabolic effects of cyclic AMP in the bivascularly perfused rat liver. *Biochem Pharmacol* **54:** 1115–1125, 1997.
6. Goresky CA, Ziegler WH and Bach GG, Capillary exchange modeling. Barrier-limited and flow-limited distribution. *Circ Res* **27:** 739–764, 1970.
7. Bracht A, Schwab AJ and Scholz R, Untersuchung von Fluβgeschwindigkeiten in der isolierten perfundierten Rattenleber durch Pulsmarkierung mit radioaktiven Substraten und mathematischer Analyse der Auswaschkinetiken. *Hoppe-Seylers Z Physiol Chem* **361:** 357–377, 1980.
8. Rodbell M and Krishna G, Preparation of isolated fat cells and fat cell "ghosts"; methods for assaying adenylate cyclase activity and levels of cyclic AMP. *Methods Enzymol* **31:** 103–114, 1974.
9. Minguetti-Câmara VC, Constantin J, Suzuki-Kemmelmeier F and Bracht A, Hepatic heterogeneity in the response to AMP studied in the bivascularly perfused rat liver. *Biochem Mol Biol Int* **44**: 693–702, 1998.
10. Bracht A, Kelmer-Bracht A, Schwab AJ and Scholz R, Transport of inorganic anions in perfused rat liver. *Eur J Biochem* **114:** 471–479, 1981.
11. Ishii EL, Schwab AJ and Bracht A, Inhibition of monosaccharide transport in the intact rat liver by stevioside. *Biochem Pharmacol* **36:** 1417–1433, 1987.
12. Castagna M, Palmer WK and Walsh DA, Metabolism of N^6,$O^{2'}$-[^{3}H]dibutyryl cyclic adenosine 3′,5′-monophosphate and macromolecular interactions of the products in perfused rat liver. *Arch Biochem Biophys* **181:** 46–60, 1977.
13. Shank RP, Adenosine 5′-monophosphate transport across the membrane of synaptosomes and myelin. *Neurochem Res* **17**: 423–430, 1992.
14. Scholz R and Bücher T, Hemoglobin-free perfusion of rat liver. In: *Control of Energy Metabolism* (Eds. Chance B, Estabrook RW and Williamson JR), pp. 393–414. Academic Press, New York, 1965.
15. Goresky CA, A linear method for determining liver sinusoidal and extravascular volumes. *Am J Physiol* **204:** 626–640, 1963.
16. Wilkinson GN, Statistical estimations in enzyme kinetics. *Biochem J* **80:** 324–332, 1961.
17. Björck Å and Dahlquist G, *Numerische Methoden*. Oldenburg Verlag, Munich, 1972.
18. Meier P and Zierler KL, On the theory of the indicator dilution method for measurement of blood flow and volume. *J Appl Physiol* **6:** 731–744, 1954.
19. Ferraresi-Filho O, Ferraresi ML, Constantin J, Ishii-Iwamoto EL, Schwab AJ and Bracht A, Transport and metabolism of palmitate in the rat liver. Net flux and unidirectional fluxes across the cell membrane. *Biochim Biophys Acta* **1103:** 239–249, 1992.
20. Ferraresi-Filho O, Ishii-Iwamoto EL and Bracht A, Transport and distribution space of octanoate in the perfused rat liver. *Cell Biochem Funct* **15:** 69–80, 1997.
21. Goresky CA, Bach GG and Rose CP, Effects of saturating metabolic uptake on space profiles and tracer kinetics. *Am J Physiol* **244:** G215–G232, 1983.
22. Coulson R, Baraniak J, Stec WJ and Jastorff B, Transport and metabolism of N6- and C8-substituted analogs of adenosine 3′,5′-cyclic monophosphate and adenosine 3′,5′-cyclic phosphorothioate by the isolated perfused rat kidney. *Life Sci* **32:** 1489–1498, 1983.
23. Krass JD, Jastorff B and Genieser HG, Determination of lipophilicity by gradient elution high-performance liquid chromatography. *Anal Chem* **69:** 2575–2581, 1997.
24. Gorin E and Brenner T, Extracellular metabolism of cyclic AMP. *Biochim Biophys Acta* **451:** 20–28, 1976.
25. Smoake JA, McMahon KL, Wright RK and Solomon SS, Hormonally sensitive cyclic AMP phosphodiesterase in liver cells. An ecto-enzyme. *J Biol Chem* **256:** 8531–8535, 1981.
26. Blecher M and Hunt NH, Enzymatic deacylation of mono- and dibutyryl derivatives of cyclic adenosine 3′,5′-monophosphate by extracts of rat tissues. *J Biol Chem* **247:** 7470–7484, 1972.
27. Houslay MD and Milligan G, Tailoring cAMP-signalling responses through isoform multiplicity. *Trends Biochem Sci* **22:** 217–224, 1997.
28. Craven P and DeRubertis FR, Reduced sensitivity of the hepatic adenylate cyclase-cyclic AMP system to glucagon during sustained hormonal stimulation. *J Clin Invest* **57:** 435–443, 1976.
29. Studer RK, Snowdowne KW and Borle AB, Regulation of hepatic glycogenolysis by glucagon in male and female rats. *J Biol Chem* **259:** 3596–3604, 1984.
30. Corvera S, Huerta-Bahena J, Pelton JT, Hruby VJ, Trivedi D and Garcia-Sáinz JA, Metabolic effects and cyclic AMP levels produced by glucagon, (1-N^{α}-trinitrophenylhistidine,12-homoarginine)glucagon and forskolin in isolated rat hepatocytes. *Biochim Biophys Acta* **804:** 434–441, 1984.